Optimized sub-wavelength grating mirror design for mid-infrared wavelength range

C. Chevallier · N. Fressengeas · F. Genty · J. Jacquet

Abstract Several designs of sub-wavelength grating mirrors adapted to mid-infrared operation are reported with several percents of tolerance for the grating fabrication. These designs have been automatically optimized by the use of a genetic-based algorithm to maximize a quality factor defined to meet the requirements of a VCSEL cavity mirror. These mirrors are devoted to integration in VCSEL operating near $\lambda = 2.3$ μm, with a large bandwidth, very high reflectivity coefficient for transverse magnetic mode only, polarization selectivity and a thickness as low as 2 μm.

1 Introduction

The existence of strong absorption lines for polluting gas (CH_4, CO_2, CO, ...) in the mid-infrared (MIR) wavelength range beyond 2 μm presents a great interest for spectroscopic measurements. Due to their particular properties, VCSELs appear as stable, compact and very efficient light sources for such an application [1, 2]. Microcavity VCSELs traditionally include two distributed Bragg mirrors (DBR), which can be fabricated with semiconductor or dielectric materials. In this wavelength range, due to a relatively low index contrast ($\Delta n \sim 0.5$), one semiconductor DBR must contain at least 20 pairs of quarter-wavelength layers to reach minimum reflectivity ($R > 99\%$) required for Room

Temperature (RT) laser operation [3]. Moreover, such reflectors usually provide bandwidths as large as 300 nm [3] but are polarization independent, which may alter the stability of emitted light by brutal polarization switches and mode competitions [4]. Furthermore, the thickness of such DBR mirrors increases with the wavelength. Since the number of layers for one DBR has to be higher than 40 to keep a high enough reflectivity and a 300 nm-large bandwidth, in the MIR range, the total thickness of VCSELs can become as high as 15 μm for an operating wavelength of $\lambda = 2.5$ μm [5], which impairs the electro-thermo-optical stability of the device.

For $\lambda \geq 2.3$ μm, the best performances were obtained with devices developed from the AlGaInAsSb semiconductor material system. Two different electrically pumped VCSEL structures, an all-epitaxial monolithic microcavity and a hybrid one, have been recently successfully developed for an emission at $\lambda \geq 2.3$ μm. The all-epitaxial monolithic structure [6] is made of two Te-doped AlAsSb/GaSb DBRs and an n^{++} InAs(Sb)/p^{++} GaSb tunnel junction. This laser structure operates at RT in a CW mode near 2.3 μm [5] and in quasi-CW (5%, 1 μs) up to 2.63 μm [7]. The hybrid structure contains a top dielectric mirror and a buried tunnel junction and operates in CW emission at RT in the 2.4 μm–2.6 μm wavelength range [8]. However, due to the absence of polarization selectivity in the structure, both of these VCSELs are likely to present hopes during laser operation.

One solution to provide a polarization selectivity is the replacement of the top cavity DBR by a sub-wavelength grating mirror (SGM) [9, 10]. Furthermore, a SGM with a low index sublayer which increases the reflectivity of the grating [11] is thinner than a DBR for an equivalently wide spectrum thus providing better electro-thermo-optical stability. Moreover, owing to its one dimensional symmetry, such a mirror provides a polarization selectivity of the reflected

C. Chevallier (✉) · N. Fressengeas · F. Genty · J. Jacquet
Laboratoire Matériaux Optiques, Photonique et Systèmes, Unité de Recherche Commune à l'Université Paul Verlaine—Metz et Supélec, 2 rue Edouard Belin, 57070 Metz, France
e-mail: christyves.chevallier@supelec.fr

light. Thus, with both these qualities, the integration of a SGM in mid-IR operating VCSELs appears as very promising to improve the beam quality and increase the wavelength of emission of such devices.

Such mirrors operate by excitation and reflection of transverse modes which propagate in the grating direction [12]. Their reflectivity is not straightforward [13] and must be numerically computed by methods such as Rigorous Coupled-Wave Analysis (RCWA) [14] or the Finite-Difference Time-Domain (FDTD) [15] method. This is the reason why the design of the SGM characteristic lengths is still an important issue [11].

In this paper, an automated optimized design of SGM mirrors for applications in the mid-IR wavelength range is proposed. The optimization is performed by the carefully definition of a quality factor which reflects the characteristics that a SGM has to meet for efficient integration in VCSEL structures. This quality factor is then optimized thanks to a genetic algorithm [16, 17]. In the following, Sect. 2 is devoted to the definition of the quality factor and the means used for its maximization, while Sect. 3 presents two different designs of Si/SiO$_2$ SGMs obtained with the previously described method and assesses their predicted performances. The two designs, with and without the use of a low index layer below SGM, have been optimized to have the largest bandwidth with a 99.9% high reflectivity centered at $\lambda = 2.3$ μm.

2 Designing and optimization of a sub-wavelength grating mirror

Reflectors designed in this work have been optimized as VCSEL top-mirrors which require high reflectivity for the widest possible bandwidth. The bandwidth was defined as the wavelength range for which the transverse magnetic mode (TM) has a reflection coefficient R_{TM} higher than 99.9%. A 99.5% value would surely have been enough to reach the laser threshold, but the remaining 0.4% was kept as a security margin to account for possible experimental growth imperfections.

In order to prevent mode hopping, the mirror must also be polarization selective. The reflection coefficient of the transverse electric mode R_{TE} was therefore set to reach a maximum value of 90% over the whole bandwidth, so as to assure the device to lase only in the TM mode. The bandwidth has also been centered at λ_0 where the VCSEL structure has been optimized.

In addition to these requirements, the mirror optimization is made under technological constraints. The first one is the photolithography resolution which limits the size of the filled and etched lengths of the grating (L_f and L_e on Fig. 1). A minimum value of 500 nm was set for each one
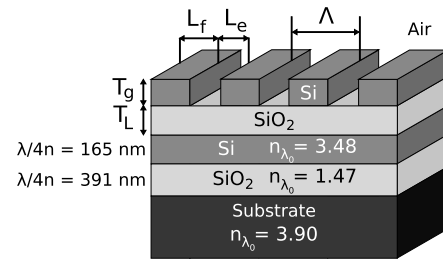

Fig. 1 Scheme of the reflector. A sub-wavelength grating mirror is combined with two quarter-wave layers to reach 99.9% reflectivity. The substrate represents the VCSEL's phase match layer. The etched length L_e, filled length L_f and thickness T_g of the grating and the sublayer thickness T_L are the free parameters which are searched to optimize the SGM for VCSEL operation

so as to ease the lithography process. The second limitation is the shape factor SF defined as the etched length L_e to grating thickness T_g ratio, which is kept at a minimum value of 0.9. This means that the optimization retains only the designs with wide grooves since a squared pattern is easier to etch than a deep one.

The simulation of the device is computed in *Sage* [18] by stable Rigorous Coupled-Wave Analysis software [14, 19] (RCWA) which finds an exact solution of Maxwell's equations for the electromagnetic diffraction problem. It is thus possible to compute the reflection efficiency of any periodic structure at the 0-order of diffraction and to numerically evaluate reflection spectra for both TM and TE mode in the mid-infrared wavelength range.
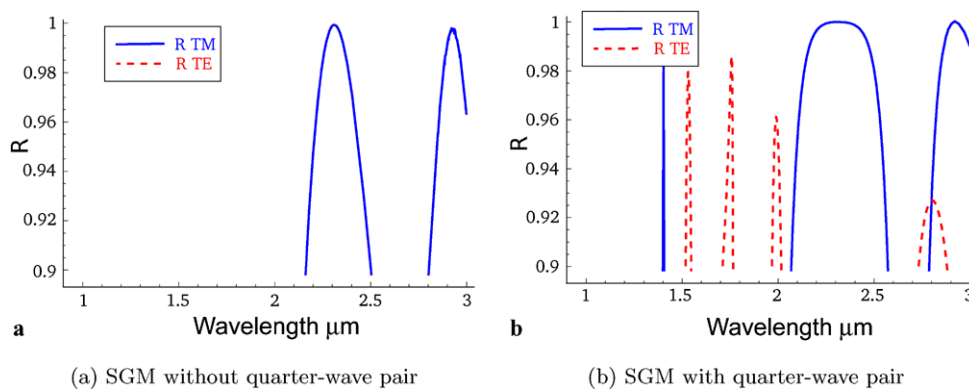
A numerical analysis of such a computed numerical spectrum can be made to quantitatively assess the mirror performances according to the above mentioned criteria. We thus propose to define the quality factor Q as follows:

$$Q = \frac{\Delta\lambda}{\lambda_0} \frac{1}{N} \sum_{\lambda=\lambda_1}^{\lambda_2} R_{TM}(\lambda)g(\lambda) \tag{1}$$

The polarization selectivity of the grating is set by selecting the range of wavelengths λ around λ_0 for which R_{TM} is higher than 99.9% and R_{TE} is lower than 90%. The centering of the bandwidth around λ_0 is made by performing a Gaussian weighted average of the R_{TM} values on the N points of the bandwidth $[\lambda_1, \lambda_2]$. The largest possible bandwidth is obtained by multiplying the latter average by the bandwidth itself $\Delta\lambda = |\lambda_2 - \lambda_1|$ in order to increase the weight of large bandwidth designs during the optimization. Q is finally normalized by λ_0.

The definition of the quality factor Q representing the performance of the mirror allows for the use of an optimization algorithm to automatically search for the best design [20]. The lengths L_e, L_f, the grating thickness T_g and the sublayer thickness T_L are the parameters of the design which are adjusted to maximize the quality. As

(a) SGM without quarter-wave pair

(b) SGM with quarter-wave pair

can be seen by performing a Newton-like optimization on Q, this optimization problem has many local maxima. Such a multimodality requires a robust and, above all, global optimization method. Genetic algorithms [16, 21] are well suited for this kind of problem since they search from a set of points which evolve from probabilistic transition rules to find an optimal solution. The use of a population of points instead of a single point decreases the chance to find a local maximum by exploring simultaneously many peaks. Another important asset of this method is the fact that no derivability condition has to be set on Q [17]. This is particularly interesting here since Q is not ensured to have derivatives everywhere over all variables. Moreover genetic algorithms use a randomized but not directionless search leading to statistically promoting the largest peaks of the Q function which represent the most tolerant designs, which is one goal of our optimization.

With the same definition of the quality factor Q, it is possible to calculate the tolerances on each dimension of the mirror. Tolerance is computed by varying one parameter at the time while keeping the other ones constant. For each value of this parameter, spectra are computed and the normalized bandwidth $\Delta\lambda/\lambda_0$ versus the length of the parameter can be plotted. The range where the mirror meets VCSEL requirements defines the interval of tolerance of the parameter, it corresponds to a non-zero value for the normalized bandwidth, i.e. when R_{TM} becomes higher than 99.9% with R_{TE} lower than 90% at λ_0.

The first optimizations of silicon ($n = 3.475$) subwavelength grating mirror with a silica ($n = 1.47$) sublayer on a GaSb substrate ($n = 3.9$) shows us too narrow bandwidths of about 20 nm (Fig. 2a) because of the optimization constraints we have set as explained above. A pair of Si/SiO$_2$ quarter-wave layer as in a DBR has been added below the SGM to increase the bandwidth and the reflectivity above 99.9% (Fig. 2b). Since this type of mirror is not polarization dependent, only one pair is used, allowing one to keep the reflectivity of the TE mode at λ_0 below the 90% threshold.

Table 1 Lengths and tolerances of the optimized mirror with a silica sublayer

	Optimum	Tolerances for $R_{TM} > 99.9\%$	
T_g	0.715 µm	0.678 µm $< T_g <$ 0.745 µm	(4.7%)
T_L	0.017 µm	0 µm $< T_L <$ 0.090 µm	
Λ	1.304 µm	1.028 µm $< \Lambda <$ 1.436 µm	(15.6%)
L_f/Λ	48%	42% $< L_f/\Lambda <$ 51%	

With this structure, two different designs have been optimized, the first one has a silica low index sublayer below the grating whereas the second one has a silicon sublayer as a phase match layer between the grating and the quarter-wave pair.
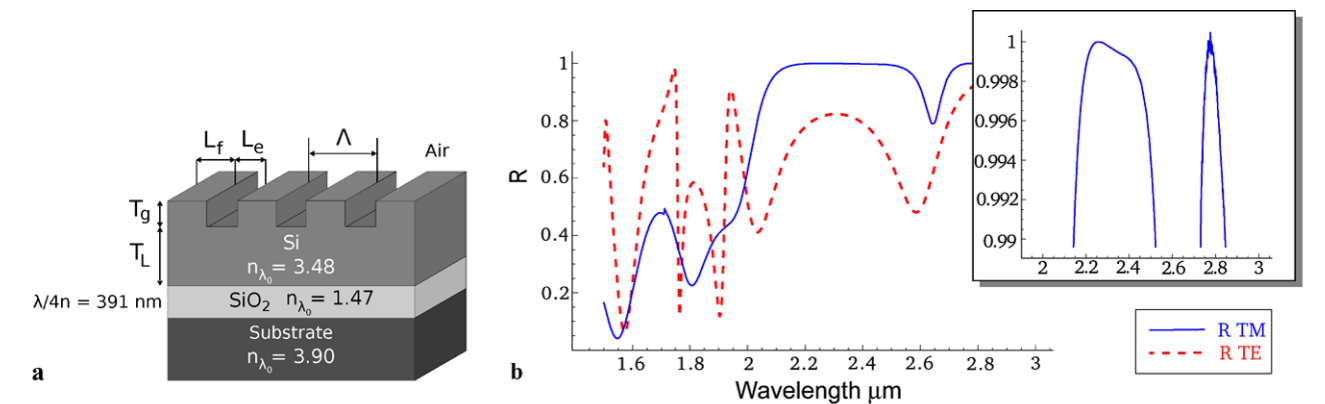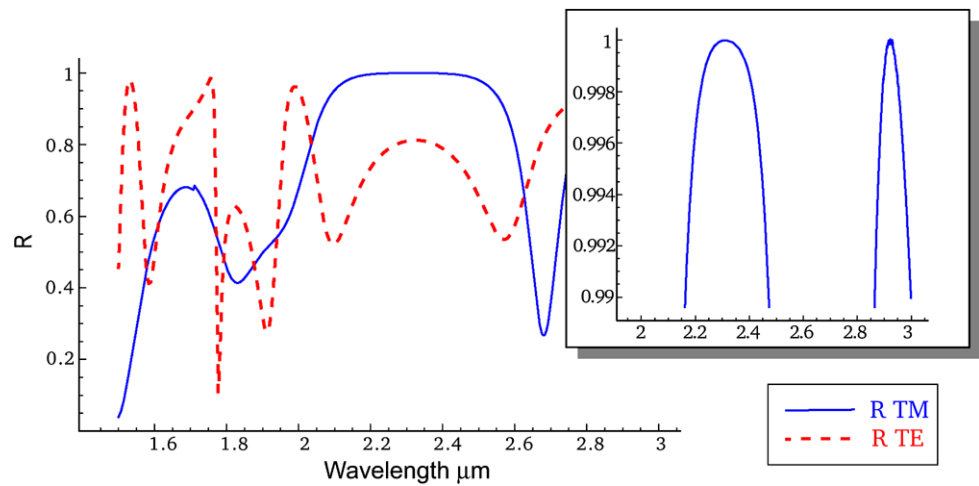
3 Optimized mirrors centered at 2.3 µm

3.1 Sub-wavelength grating mirror with a silica sublayer

The reflector presented on Fig. 1 is a combination of a subwavelength grating of silicon and two quarter-wave layers of silicon and silica which increase the reflectivity to very high values of 99.9%. The SGM is on top of a silica low index layer as described in [11]. The choice of silicon is made in regard to its well known properties and ease to process. The substrate corresponds to the GaSb match layer of the final VCSEL with an optical index of 3.9. During the optimization, the pattern sizes L_e and L_f are allowed to vary between 0.5 µm and 1 µm while thicknesses T_g and T_L are only limited below 1 µm. These are severe constraints for the optimization algorithm which would rather lead to thinner patterns of less than 260 nm for a small shape factor SF of less than 0.4 [11].

The optimization returns a design (Table 1) with a grating thickness T_g of 0.715 µm for a filled length L_f of 0.629 µm and an etched length L_e of 0.675 µm. This design respects the technological constraints with patterns longer

Fig. 3 Reflection spectra of
TM (*solid blue*) and TE (*dashed
red*) mode of the silica sublayer
mirror with a 152 nm bandwidth

(a) Scheme of the mirror with silicium as a
phase match layer between the grating and
the quarter-wave layer.

(b) Reflection spectra of TM *(solid blue)* and TE *(dashed red)* mode with a
206 nm bandwidth.

Fig. 4 Second design with a silicon sublayer

than 0.500 μm and a shape factor *SF* of 0.94. The silica sub-
layer has a thickness T_L of only 17 nm, but this length has
the best tolerance and does not significantly affect the qual-
ity of the mirror while it is kept thinner than 90 nm. The
spectra of this mirror (Fig. 3) show us a 152 nm bandwidth
mirror ($\Delta\lambda/\lambda_0 = 6.6\%$) centered at 2.315 μm. The R_{TM} co-
efficient reaches very high values above 99.9%, whereas
R_{TE} is kept below 80%. Such a mirror satisfies all of our
requirements for a VCSEL application.

This design gives a very high reflective and polarized
mirror with a large bandwidth. In addition to these qualities,
the optimization found a very tolerant design with between
4% and 15% of error allowed on each dimension.

However, it can be noticed that the optimization suggests
that the silica sublayer be as thin as possible. Therefore, and
though it impairs the use of a selective etching process, we

have tried our optimization method on a second design from
which the silica sublayer has been removed (Fig. 4a).

3.2 Sub-wavelength grating mirror with a silicon sublayer

This leads to a design where the silica sublayer is replaced
by a silicon one as a phase match layer between the grating
and the quarter-wave layers. The optimization is performed
under the same conditions and results in a 0.700 μm thick
grating with a 0.635 μm etched length L_e and 0.601 μm
filled length L_f (Table 2). The thickness of the silicon sub-
layer is 0.201 μm. This design has higher tolerance values
up to 34% and a larger bandwidth of 206 nm ($\Delta\lambda/\lambda_0 = 9\%$)
centered at $\lambda_0 = 2.303$ μm as shown on Fig. 4b.

Despite higher tolerances and the absence of nanometric
sublayer, this second mirror requires one to precisely con-

trol the etching process since the shape factor is smaller ($SF = 0.9$) and no selective etching method can be used.

3.3 Influence of the grating period on the quality of the mirrors

The computation of the tolerance allows the study of the influence of parameters of the design on the mirror quality. We have chosen to present the influence of the grating period which highlights two different phenomena. On Fig. 5, the normalized bandwidth $\Delta\lambda/\lambda_0$ is plotted versus the grating period Λ for R_{TM} thresholds of 99.9% and 99.99%. The grating period varies from 1 µm to 1.5 µm, which is the range for which the SGM has a 99.9% high bandwidth. The others parameters of the design are kept at their optimal values (Tables 1 and 2). The arrow on the graphs points the optimized grating period presented previously.

For both designs, the quality of the mirror increases for periods shorter than the optimal one. The mirror with a silica sublayer presents a bandwidth (Fig. 5a) as large as 335 nm for a 1.068 µm period ($\Delta\lambda/\lambda_0 = 14.9\%$), which is more than twice the values found by the optimization. The reason why such designs are not retained by the optimization algorithm is that they have smaller etched lengths, here

Table 2 Lengths and tolerances of the optimized mirror with a silicon sublayer

	Optimum	Tolerances for $R_{TM} > 99.9\%$	
T_g	0.700 µm	0.679 µm $< T_g <$ 0.741 µm	(4.4%)
T_L	0.201 µm	0.119 µm $< T_L <$ 0.256 µm	(34%)
Λ	1.236 µm	1.037 µm $< \Lambda <$ 1.500 µm	(19%)
L_f/Λ	49%	47% $< L_f/\Lambda <$ 53%	

$L_e = 0.553$ µm, and since the grating thickness T_g is kept at its optimal value of 0.715 µm, the shape factor SF becomes as low as 0.77, which is forbidden by our constraints. This confirms that constraints are severe and better performing designs can be found with a smaller shape factor [11].

The second phenomenon is that the bandwidth becomes higher than 99.99% for longer periods. Figure 5b exhibits a 30 nm bandwidth for a 1.322 µm period SGM with a silicon sublayer for $R_{TM} > 99.99\%$. This shows that the bandwidth can reach higher reflective values at λ_0 with an adjusted design, but for a narrower bandwidth since its width at $R_{TM} = 99.9\%$ is only of 121 nm which is 80 nm less than the optimal value. This point demonstrates that our program really searches for the widest possible bandwidth for a precise R_{TM} value.

4 Conclusion

In this paper, two SGM mirrors as thin as 2 µm and exhibiting the required properties for a VCSEL integration at $\lambda = 2.3$ µm were presented. These mirrors combine a large bandwidth of more than 150 nm with a polarization selectivity by keeping R_{TE} below 0.8 in the wavelength range where the VCSEL would operate. With the definition of a quality factor of VCSEL mirrors, the design optimization process is automated and can be easily performed under technological constraints. This factor also allows the computation of tolerances which are higher than 4 percent on the different lengths for which the mirrors should be easy to produce. The integration of such SGM mirrors in mid-IR emitting VCSELs would improve their emission properties allowing the fabrication of CW operating devices above 2.3 µm.
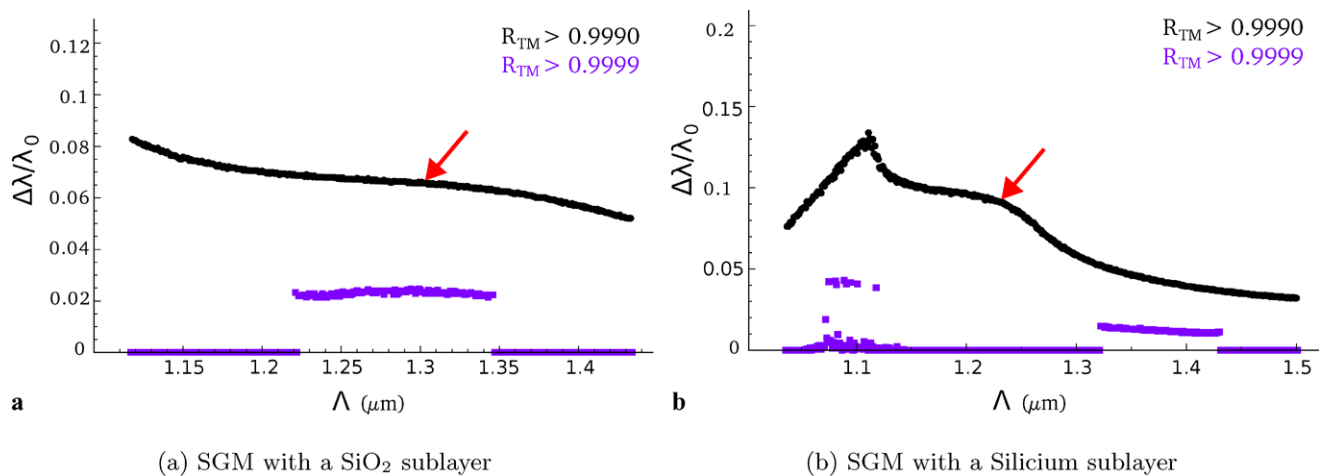

(a) SGM with a SiO$_2$ sublayer

(b) SGM with a Silicium sublayer

Fig. 5 Tolerance of the grating period: normalized bandwidth $\Delta\lambda/\lambda_0$ vs. grating period Λ for a R_{TM} threshold of 99.9% (*black*) and 99.99% (*purple*). The *arrow* indicates the design found by the optimization algorithm

References

1. A. Hangauer, J. Chen, R. Strzoda, M. Ortsiefer, M.-C. Amann, Wavelength modulation spectroscopy with a widely tunable InP-based 2.3 μm vertical-cavity surface-emitting laser. Opt. Lett. **33**(14), 1566–1568 (2008)

2. J. Chen, A. Hangauer, R. Strzoda, M.C. Amann, VCSEL-based calibration-free carbon monoxide sensor at 2.3 μm with in-line reference cell. Appl. Phys. B (2010). 10.1007/s00340-010-4011-0

3. A. Perona, A. Garnache, L. Cerutti, A. Ducanchez, S. Mihindou, P. Grech, G. Boissier, F. Genty, AlAsSb/GaSb doped distributed Bragg reflectors for electrically pumped VCSELs emitting around 2.3 μm. Semicond. Sci. Technol. **22**(10), 1140–1144 (2007)

4. A. Ouvrard, A. Garnache, L. Cerutti, F. Genty, D. Romanini, Single-frequency tunable sb-based VCSELs emitting at 2.3 μm. IEEE Photon. Technol. Lett. **17**(10), 2020–2022 (2005)

5. L. Cerutti, A. Ducanchez, G. Narcy, P. Grech, G. Boissier, A. Garnache, E. Tournié, F. Genty, GaSb-based VCSELs emitting in the mid-infrared wavelength range (2–3 μm) grown by MBE. J. Cryst. Growth **311**(7), 1912–1916 (2009)

6. L. Cerutti, A. Ducanchez, P. Grech, A. Garnache, F. Genty, Room-temperature, monolithic, electrically-pumped type-l quantum-well Sb-based VCSELs emitting at 2.3 μm. Electron. Lett. **44**(3), 203–205 (2008)

7. A. Ducanchez, L. Cerutti, P. Grech, F. Genty, E. Tournié, Mid-infrared GaSb-based EP-VCSEL emitting at 2.63 μm. Electron. Lett. **45**(5), 265–267 (2009)

8. A. Bachmann, S. Arafin, K. Kashani-Shirazi, Single-mode electrically pumped GaSb-based VCSELs emitting continuous-wave at 2.4 and 2.6 μm. New J. Phys. **11**(12), 125014 (2009)

9. M.C.Y. Huang, Y. Zhou, C.J. Chang-Hasnain, A surface-emitting laser incorporating a high-index-contrast subwavelength grating. Nat. Photon. **1**(2), 119–122 (2007)

10. I. Chung-Sung, J. Mork, P. Gilet, A. Chelnokov, Subwavelength grating-mirror VCSEL with a thin oxide gap. IEEE Photon. Technol. Lett. **20**, 105–107 (2008)

11. C.F.R. Mateus, M.C.Y. Huang, Y. Deng, A.R. Neureuther, C.J. Chang-Hasnain, Ultrabroadband mirror using low-index cladded subwavelength grating. IEEE Photon. Technol. Lett. **16**(2), 518–520 (2004)

12. F. Brückner, D. Friedrich, T. Clausnitzer, M. Britzger, O. Burmeister, K. Danzmann, E.B. Kley, A. Tünnermann, R. Schnabel, Realization of a monolithic high-reflectivity cavity mirror from a single silicon crystal. Phys. Rev. Lett. **104**(16), 163903 (2010)

13. R. Magnusson, M. Shokooh-Saremi, Physical basis for wideband resonant reflectors. Opt. Express **16**(5), 3456–3462 (2008)

14. M.G. Moharam, Drew A. Pommet, Eric B. Grann, T.K. Gaylord, Stable implementation of the rigorous coupled-wave analysis for surface-relief gratings: enhanced transmittance matrix approach. J. Opt. Soc. Am. A **12**(5), 1077–1086 (1995)

15. K. Yee, Numerical solution of initial boundary value problems involving maxwell's equations in isotropic media. IEEE Trans. Antennas Propag. **14**(3), 302–307 (1966)

16. D. Goodman, Galileo 1.0b. http://sourceforge.net/projects/galileo/, February 2003

17. D.E. Goldberg, *Genetic Algorithms in Search, Optimization and Machine Learning* (Addison-Wesley Longman, Boston, 1989)

18. W.A. Stein, Sage mathematics software (version 4.3). http://www.sagemath.org/, February 2010. The Sage Group

19. H. Rathgen, Mrcwa 20080820. http://mrcwa.sourceforge.net/, February 2010

20. J. Wang, Y. Jin, J. Shao, Z. Fan, Optimization design of an ultrabroadband, high-efficiency, all-dielectric grating. Opt. Lett. **35**(2), 187–189 (2010)

21. D.L. Kroshko, OpenOpt 0.27. http://openopt.org/, December 2009